SCIENCE CHINA
Earth Sciences

• RESEARCH PAPER •

November 2011 Vol.54 No.11: 1779–1788
doi: 10.1007/s11430-011-4282-2

Features of rainfall and latent heating structure simulated by two convective parameterization schemes

WANG XiaoCong[1,2,3], BAO Qing[1], LIU Kun[3], WU GuoXiong[1] & LIU YiMin[1*]

[1]*State Key Laboratory of Numerical Modeling for Atmospheric Sciences and Geophysical Fluid Dynamics (LASG), Institute of Atmospheric Physics, Chinese Academy of Sciences, Beijing 100029, China;*
[2]*Graduate University of Chinese Academy of Sciences, Beijing 100049, China;*
[3]*Numerical Weather Prediction Center, China Meteorological Administration, Beijing 100081, China*

Received December 2, 2010; accepted April 12, 2011; published online September 9, 2011

Using the latest version of SAMIL (Spectral Atmosphere Model of IAP LASG) developed by LASG/IAP, we evaluate the model performance by analyzing rainfall, latent heating structure and other basic fields with two different convective parameterization schemes: Manabe Scheme and Tiedtke Scheme. Results show that convective precipitation is excessively overestimated while stratiform precipitation is underestimated by Tiedtke scheme, thus causing less stratiform rainfall proportion compared with TRMM observation. In contrast, for Manabe scheme stratiform rainfall belt is well simulated, although precipitation center near Bay of Bengal (BOB) spreads eastward and northward associated with unrealistic strong rainfall downstream of the Tibet Plateau. The simulated latent heating structure indicates that Tiedtke scheme has an advantage over Manabe scheme, as the maximum convective latent heating near middle of troposphere is well reproduced. Moreover, the stratiform latent heating structure is also well simulated by Tiedtke scheme with warming above freezing level and cooling beneath freezing level. As for Manabe scheme, the simulated maximum convective latent heating lies near 700 hPa, lower than the observation. Additionally, the warming due to stratiform latent heating extends to the whole vertical levels, which is unreasonable compared with observation. Taylor diagram further indicates that Tiedtke scheme is superior to Manabe scheme as higher correlation between model output and observation data is achieved when Tiedtke scheme is employed, especially for the temperature near 200 hPa. Finally, a possible explanation is addressed for the unrealistic stratiform rainfall by Tiedtke scheme, which is due to the neglect of detrained cloud water and cloud ice during convective process. The speculation is verified through an established sensitivity experiment.

Manabe scheme, Tiedtke scheme, stratiform rainfall, convective rainfall, latent heating, SAMIL

Citation: Wang X C, Bao Q, Liu K, et al. Features of rainfall and latent heating structure simulated by two convective parameterization schemes. Sci China Earth Sci, 2011, 54: 1779–1788, doi: 10.1007/s11430-011-4282-2

In realistic atmosphere, cumulus convection and its interaction with large scale circulation have an important impact on the climate changes. Not only precipitation but also cloud radiation forcing is influenced by cumulus convection. It also has a profound impact on the vertical structure of temperature and moisture due to its powerful ascending motion. Cumulus parameterization remains a challenge for meteorologists, although significant progresses have been made through the last 40 years. Since the first convection scheme proposed by Smagorinsky [1] was successfully applied in numerical model, three typical convection schemes have been developed: (1) Manabe adjustment scheme [2], (2) Kuo scheme based on moisture convergence [3], and (3) Arakawa Mass flux scheme [4], which was further simplified by Tiedtke [5] under bulk assumption.

The importance of cumulus convection cannot be over-

*Corresponding author (email: lym@lasg.iap.ac.cn)

emphasized, and the performance of cumulus parameterization schemes is of great concern. For numerical weather models, the simulation of synoptic process is mostly concerned [6] whereas for climate models, interests focus on the simulated precipitation and atmosphere circulation [7, 8]. Liu et al. [9] studied the sensitivity of ITCZ by employing different cumulus schemes based on an aquaplanet configuration. Besides, the successful simulation of ENSO as well as MJO is dependent largely on the convective schemes [10, 11]. Cumulus convection can also have impacts on atmospheric radiation process by changing radiation flux, thus affecting local energy budget [12]. Moreover, mass flux convection schemes, capable of transporting passive tracers in vertical direction, are more meticulous and remarkable [13].

Recently, Lin et al. [14] suggested that diabatic heating induced by stratiform precipitation also plays an important role in the simulation of MJO. The profile of total heating in convection regions is top-heavy or centered high in the upper troposphere, which is caused by vertical dipole heating profiles with heating in the upper troposphere and cooling in the lower troposphere. Thus, to some extent, the simulation of MJO depends on the simulated convective and stratiform precipitation.

In this work, we compare both convective and large-scale precipitation using two different cumulus schemes with TRMM satellite data as a reference. Furthermore, the latent heating structure simulated by two schemes is analyzed. Utilizing ERA40 and NCEP/NCAR reanalysis data, we evaluate the overall performance of our latest model, in which the two cumulus schemes are employed respectively. The motivation of this study is to find out the deficiencies of the current model as well as corresponding possible solutions.

1 Model and data

The model used in this study is a latest version of SAMIL, an atmospheric component of the Flexible Global Ocean-Atmosphere-Land System (FGOALS) developed by the State Key Laboratory of Atmospheric Sciences and Geophysical Fluid Dynamics/Institute of Atmospheric Physics (LASG/IAP) [15]. The dynamical framework adopted is a hybrid-coordinate system with 26 vertical layers (L26), and rhomboidally truncated at wave-number 42 in the horizontal (R42), roughly 2.8°×1.66° Gaussian grid [16–19]. Various grid and sub-grid scale parameterization schemes are included in the physical package of SAMIL, such as convection, radiation, cloud generation (dissipation), land surface process and so on [20–24]. A detail introduction about SAMIL can be found in Zhou et al. [25]. For cumulus convection, a mass flux scheme proposed by Tiedtke is introduced, and is substituted for the previous Manabe adjustment scheme [26]. Overall, the improved model has a better ability in the simulation of rainfall as well as East Asian Monsoon. However, some problems still exist, such as the double ITCZ in the central-western Pacific, cold and dry biases in the middle troposphere. The double ITCZ problem is effectively alleviated after several modifications to the shallow convection scheme [27]. Nevertheless, it is necessary to have a comprehensive evaluation of the current model in order to make a further improvement.

For Manabe scheme, the convection is triggered when the lapse rate of a saturated area tends to exceed the moist adiabatic lapse rate. The moist static energy is assumed to be conserved during the adjustment, and thus the following equations hold

$$\frac{\partial}{\partial p}\theta_e(\hat{T},\hat{q},p)=0, \tag{1}$$

$$\int_{p_B}^{p_T}[c_p(\hat{T}-T)+L(\hat{q}-q)]\mathrm{d}p=0, \tag{2}$$

where θ_e, T, q refers to potential temperature, temperature, and specific humidity before adjustment; $\hat{T}$, $\hat{q}$ ($\hat{q}=p_S(\hat{T},p)$) stands for temperature and specific humidity after adjustment.

Tiedtke scheme is a comprehensive mass flux scheme, in which three types of convection are considered, such as penetrative convection in connection with large-scale convergent flow, shallow convection in suppressed conditions like trade wind cumuli, and middle convection like extra-tropical organized convection. The contributions of cumulus convection to the large-scale heat and moisture are described as

$$\frac{\partial\overline{s}}{\partial t}=-\frac{1}{\overline{\rho}}\frac{\partial}{\partial z}[M_u s_u+M_d s_d-(M_u+M_d)\overline{s}]+L(c_u-e_d-\tilde{e}_l-\tilde{e}_p), \tag{3}$$

$$\frac{\partial\overline{q}}{\partial t}=-\frac{1}{\overline{\rho}}\frac{\partial}{\partial z}[M_u q_u+M_d q_d-(M_u+M_d)\overline{q}]-(c_u-e_d-\tilde{e}_l-\tilde{e}_p), \tag{4}$$

where s, q stands for dry static energy and specific humidity; M_u, M_d, C_u and e_d are the net contributions from all clouds to the upward mass flux, downward mass flux, condensation and evaporation, respectively, s_u, s_d, q_u and q_d are the weighted averages of s and q from all updrafts and downdrafts. The over bar denotes averages over a horizontal area that is large enough to contain an ensemble of cumulus clouds.

For deep convection, the adjustment closure suggested by Nordeng [28] is adopted, which relates the cloud base mass flux to the degree of convective instability, as expressed in terms of CAPE (Convective Available Potential Energy).

$$CAPE = \int \left(\frac{g}{\overline{T}_v}(T_v - \overline{T}_v) - gl \right) \mathrm{d}z, \tag{5}$$

$$\frac{\partial CAPE}{\partial t} \approx -\int \frac{g}{\overline{T}_v} \frac{\partial \overline{T}_v}{\partial t} \mathrm{d}z \approx -M_B \int \left(\frac{(1+\delta\overline{q})}{c_p \overline{T}_v} \frac{\partial \overline{s}}{\partial z} + \delta \frac{\partial \overline{q}}{\partial z} \right) \eta \frac{g \mathrm{d}z}{\overline{\rho}}, \tag{6}$$

where η is the normalized vertical profile of the sub-ensemble mass flux. For shallow convection, a moisture convergence closure suggested by Tiedtke is employed where the moisture content in the Planetary Boundary Layer (PBL) between the surface and cloud base is assumed to be stationary, allowing cloud base to be determined from moisture convergence including surface fluxes.

The large-scale condensation scheme is parameterized as

$$\hat{q}_k = q_k^* + \frac{\mathrm{d}q_k^*}{\mathrm{d}T}(\hat{T}_k - T_k), \tag{7}$$

$$\hat{T}_k = T_k + \frac{L}{c_p}(q_k - \hat{q}_k). \tag{8}$$

Thus, combining eqs. (7) and (8), we get

$$\hat{q}_k = \left(q_k^* + q_k \frac{L}{c_p} \frac{\mathrm{d}q_k^*}{\mathrm{d}T} \right) \Big/ \left(1 + \frac{L}{c_p} \frac{\mathrm{d}q_k^*}{\mathrm{d}T} \right), \tag{9}$$

where T_k, q_k, q_k^* stands for temperature, specific humidity, and saturated specific humidity before adjustment; $\hat{T}_k$, $\hat{q}_k$ denotes temperature and specific humidity after adjustment.

The model is integrated for 25 years under two cumulus schemes and the average output of last ten years are used for analysis. The verification data used in this study consisted of (1) GPCP (Global Precipitation Climatology Project) [29]; (2) CMAP [30]; (3) TRMM-3A12 (Tropical Rainfall Measuring Mission); (4) TRMM-3A25; (5) ERA40 [31]; and (6) NCEP/NCAR reanalysis [32].

2 Precipitation

Precipitation is a good criterion to reveal the merits of model dynamical core and physics package, in which the cumulus parameterization scheme is particularly important. In order to objectively evaluate the cumulus schemes, two types of TRMM data are used as a reference. One is TRMM-3A12 based on TMI (TRMM Microwave Image) and the other is TRMM-3A25 based on TRMM-PR (TRMM Precipitation Radar). Figure 1 presents the observed and simulated distribution of summer convective rainfall in tropical regions. The TRMM observation indicates a strong rain belt along the north ITCZ with the maximum center lying at BOB, SC (South China) and warm pool of West Pacific. In contrast, the precipitation is weaker in south of the equator. Moreover, the rainfall strength reflected by TRMM-3A25 is slightly less than that by TRMM-3A12, with a mean precipitation rate about 3 mm/d. As shown in Figure 1(d), Tiedtke scheme can well reproduce the observed rainfall centers, although the precipitation in Philippines is artificially extended northward. On the contrary, for Manabe scheme the precipitation center in Philippines is well simulated, but precipitation in BOB spreads eastward and northward associated with unrealistic strong rainfall downstream of the Tibet Plateau. As to the rainfall intensity, more precipitation is simulated by both schemes in comparison with TRMM observation. Overall, the simulation by Manabe scheme seems slightly more reasonable. The failure of Tiedtke scheme is probably due to the following reasons: (1) The threshold of the scheme is strict; thus weak convection is suppressed while more precipitation is produced once the threshold is satisfied, as more accumulated energy is released. (2) Convective precipitation is also affected by stratiform rainfall process. (3) The important air-sea interaction is ignored in the experiments [33].

Figure 2 shows the observed and simulated distribution of summer stratiform rainfall in tropics. The pattern of observed stratiform rainfall is much similar to that of convective rainfall displayed in Figure 1(a) and (b). Houze [34] suggested cumulonimbus clouds in tropics contain an evolving pattern of newer and older precipitation. In regions of older convection, the vertical air motions are generally weaker, with the particles increasing their mass by vapor diffusion, which are stratiform echoes on radar [34–36]. As shown in Figure 2(c), the distribution of stratiform rainfall is well simulated by Manabe scheme, though the intensity is slightly overestimated. However, Tiedtke scheme fails in reproducing the observed precipitation pattern. The simulated stratiform precipitation rate along ITCZ is less than 0.2 mm/d, much weaker than the observed. Conversely, in East Pacific and Atlantic Oceans where subtropical high prevails, moderate stratiform rain is artificially produced, which is also simulated by Manabe scheme. The poor performance in east oceans is probably due to the low cloud scheme, for which a traditional diagnostic method is still used.

The contrast between Figure 1(d) and Figure 2(d) indicates that convective precipitation is overestimated while stratiform precipitation is underestimated by Tiedtke scheme. Figure 3 presents the observed and simulated proportion of stratiform rainfall. In subtropical regions where frontal precipitation primarily occurs, the observed proportion reveals a high level above 50%. In equatorial areas, the observed proportion reaches as high as 40% in either summer or winter and is even higher reflected by TRMM-3A25, approaching 50%, which was also demonstrated by Cheng [37]. It was once generally thought that stratiform precipitation was occurring primarily in middle latitudes—in baroclinic cyclones and fronts. Since most clouds in the tropics

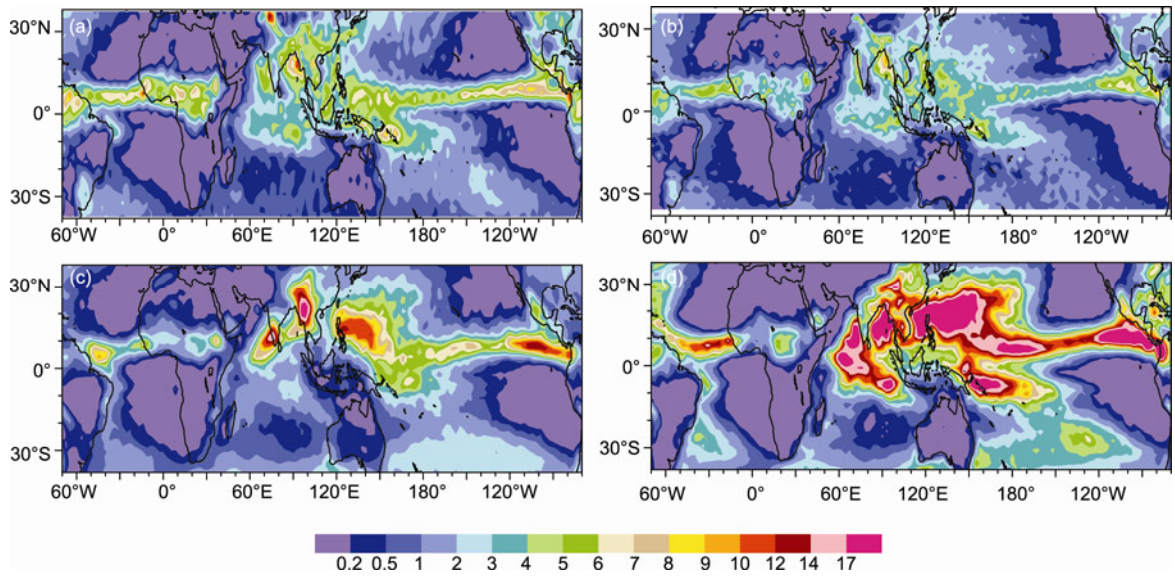

Figure 1 Tropical convective rainfall in summer (JJA). (a) TRMM-3A12; (b) TRMM-3A25; (c) Manabe scheme; (d) Tiedtke scheme (unit: mm/d).

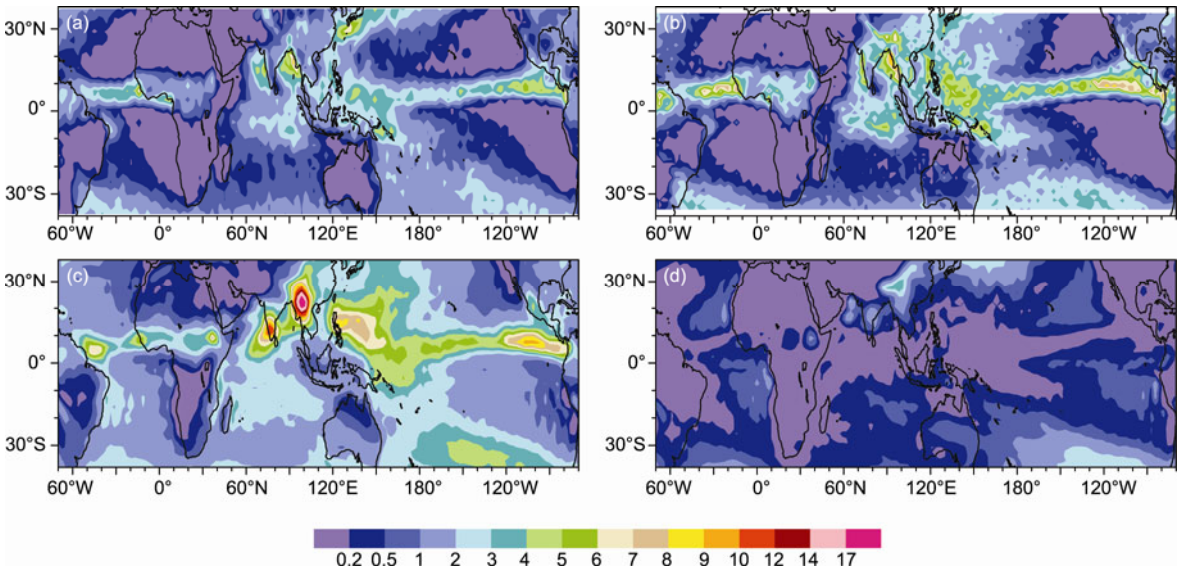

Figure 2 Tropical stratiform rainfall in summer (JJA). (a) TRMM-3A12; (b) TRMM-3A25; (c) Manabe scheme; (d) Tiedtke scheme (unit: mm/d).

are convection-generated cumulonimbus, the precipitation in these regions is taken as convective rainfall. However, radar observations showed large radar echoes composed of convective rain alongside stratiform precipitation, with the stratiform echoes covering great areas and accounting for a large portion of the total rainfall. As shown in Figure 3(g)–(i), the simulated proportion of stratiform rainfall in tropical oceans is well reproduced by Manabe scheme, but excessively overestimated in mid latitudes. In contrast, for Tiedtke scheme more convective and less stratiform rainfall leads to a lower value of stratiform rainfall proportion, less than 10% in most regions.

At first, the underestimated stratiform rainfall by Tiedtke scheme is thought to be caused by the cumulus parameterization scheme, as more water vapor is deemed to be consumed during convective process. Nevertheless, the problem persists even if large-scale condensation scheme is firstly employed. At last, the reason is figured out and it comes from the unmatched stratiform rainfall scheme, which completely ignored the detrained cloud water and cloud ice produced during cumulus convective process [38]. In fact, the detrained water substance is a significant source of precipitation, which can never be neglected. The well simulated stratiform rainfall by Manabe scheme is attributed to the matched convective and stratiform schemes, as both are essentially adjustment schemes based on the conserva-

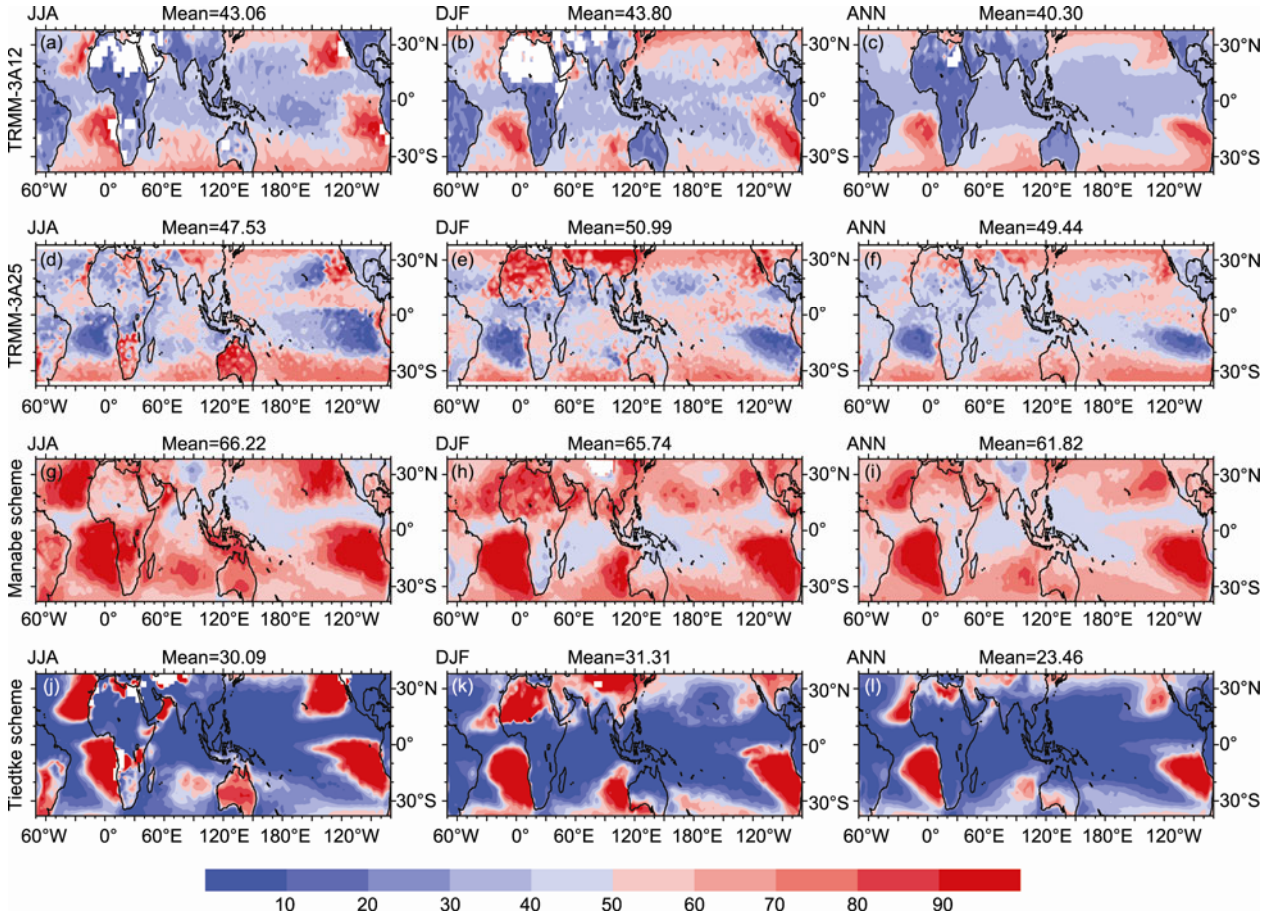

Figure 3 Stratiform rainfall proportion (unit: %).

tion of moist static energy.

Figure 4 gives the annual cycle of zonally averaged stratiform precipitation, convective precipitation, and total precipitation. As shown in Figure 4(a)–(f), the observed spatial and temporal distribution of stratiform precipitation is similar to that of convective precipitation. Rain bands begin moving northward in spring and reach the northernmost in summer. Afterwards, rain belt starts retreating and returns to the south of equator in winter. For convective and total precipitation, the rainfall shift with seasons is well reproduced, although the intensity is overestimated, especially for Tiedtke scheme. As for stratiform precipitation, Tiedtke scheme fails in reproducing the observed annual cycle while the simulation by Manabe scheme is much closer to the observation.

3 Latent heating

The diabatic heating is one of the most important energy for air movement and atmosphere circulation changes. In tropic regions, the latent heating induced by precipitation is a significant component, which has a great impact on the formation and variation of the subtropical high [39] as well as the intra-seasonal oscillation. Figure 5 shows the vertical profile of latent heating induced by convective and stratiform precipitation in equatorial regions (5°S–5°N). The convective heating center is located in Indian monsoon regions and West Pacific Ocean, where convective precipitation primarily occurs. The stronger convective heating simulated by Tiedtke scheme is due to the overestimated convective precipitation. Moreover, the altitude of maximum heating lies near 500 hPa by Tiedtke scheme and below 600 hPa by Manabe scheme. For Manabe scheme, the stratiform heating intensity is similar to that by convective precipitation, with the maximum heating lying near 400 hPa. As displayed in Figure 5(d), the stratiform heating by Tiedtke scheme is much weaker, with moderate warming above 400 hPa and cooling below 600 hPa. It is worth noting that artificial heating appears near 900 hPa in both schemes, which is probably related to the underestimated evaporation of rainfall above surface layer.

Theoretical studies within the wave-heating feedback framework, the important mechanism for MJO [40], suggest that the profile of heating is important to the strength and propagation of disturbances. Lin et al. [14] found that con-

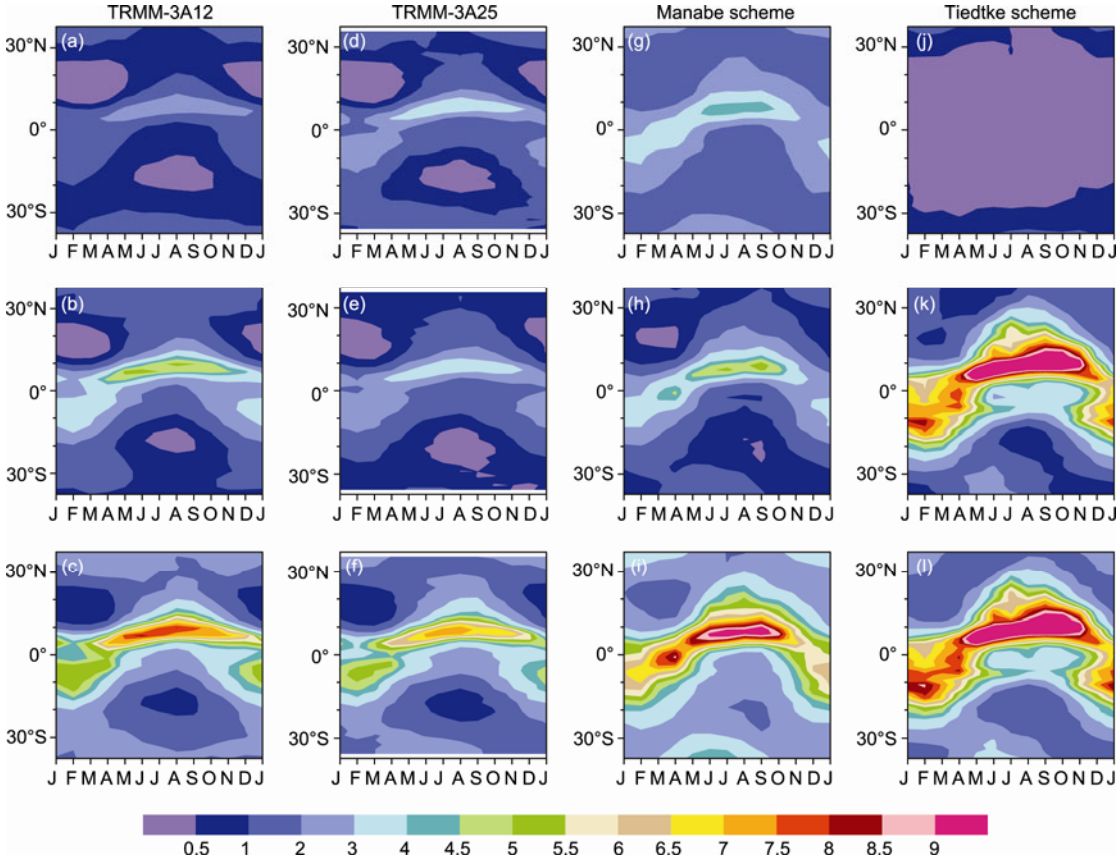

Figure 4 Temporal and spatial distribution of stratiform rainfall, convective rainfall and total rainfall (unit: mm/d).

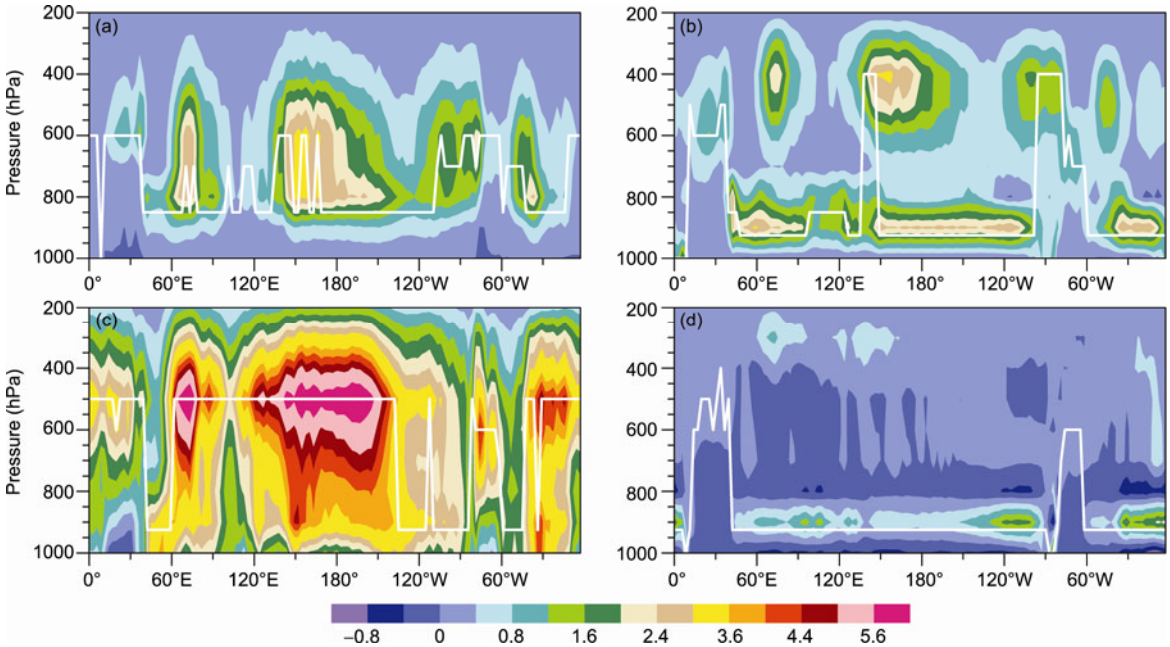

Figure 5 Latent heating structures (5°S–5°N). (a) Convective and (b) stratiform by Manabe scheme; (c) convective and (d) stratiform by Tiedtke scheme. The white curves stand for height of maximum heating (unit: K/d).

vective heating exists widely in the troposphere and peaks in the middle troposphere near the 0°C level. The stratiform heating, however, is characterized by heating in the upper troposphere and cooling in the lower troposphere. Figure 6(a) and (b) gives the profile of convective and stratiform heating by Manabe scheme during the wet phase of MJO in West Pacific Ocean (5°N–5°S, 145°E–155°E). The simulated convective heating is positive above 900 hPa, with the maximum lying near 700 hPa, lower than the observation. As for stratiform heating, Manabe scheme fails in reproducing the vertical dipole heating profile, but with a behavior of moderate heating in the whole troposphere. The two kinds of latent heating simulated by Tiedtke scheme are displayed in Figure 6(c) and (d). The latent heating structure shows that Tiedtke scheme has an advantage over Manabe scheme as the maximum convective latent heating near middle of troposphere is well reproduced. Besides, the stratiform latent heating structure is also well simulated with warming above freezing level and cooling beneath freezing level. The heating intensity indicates that convective heating is much stronger than stratiform heating, almost ten times or so, mainly owing to the excessively overestimated convective precipitation.

4 Atmosphere circulation fields

Analysis of latent heating structure indicates that Tiedtke scheme is better than Manabe scheme, although the simulated rainfall seems worse, especially for stratiform precipitation. As latent heating is tightly related with specific humidity and temperature, it is necessary to comprehensively assess the performance of two cumulus schemes by evaluating atmosphere circulation fields.

Taylor Diagram [41] is used here to quantitatively reveal the similarity between the observed and simulated fields. Two types of observation data are utilized here: one is ERA40 (Figure 7(a), (b)), and the other is NCEP/NCAR reanalysis (Figure 7(c), (d)). For winter, the obtained correlation coefficient is higher when Tiedtke scheme is employed, especially for the temperature of upper troposphere. Overall, the correlation coefficient is approaching 80% for Tiedtke scheme and below 60% for Manabe scheme. Moreover, the obtained standard deviation is near 1.0 for Tiedtke scheme and about 1.5 for Manabe scheme. The temperature of upper troposphere is influenced largely by cloud-radiation process, which is closely linked with convective process. As discussed in Section 3, Tiedtke scheme is superior to Manabe scheme in the simulation of latent

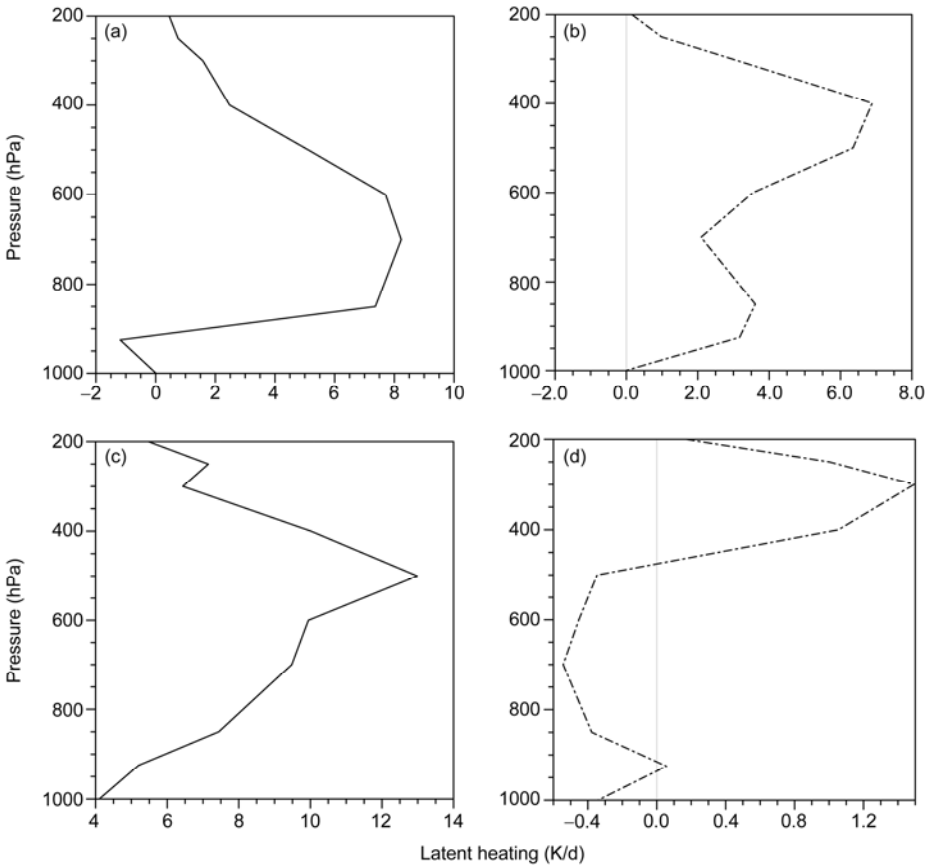

Figure 6 The profiles of latent heating during wet phase of MJO. (a) Convective and (b) stratiform by Manabe scheme; (c) convective and (d) stratiform by Tiedtke scheme (unit: K/d).

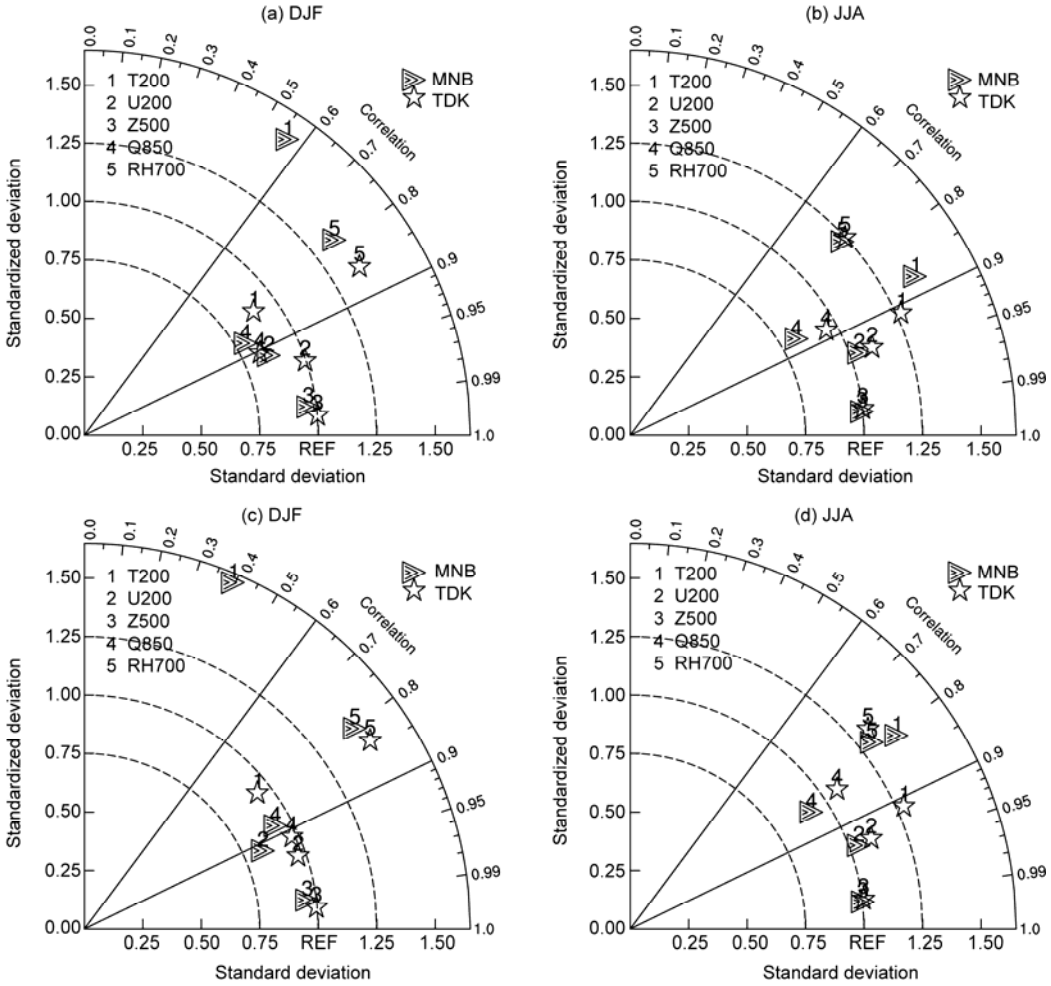

Figure 7 Correlation ships between observation and simulation for winter (a) REF: ERA40, (c) REF: NCEP, and for summer (b) REF: ERA40, (d) REF: NCEP. MNB: Manabe scheme; TDK: Tiedtke scheme.

heating structure, which may be explained for the well simulated temperature by Tiedtke scheme. For summer, the general performance of Tiedtke scheme is still better than that of Manabe scheme, especially for the zonal wind at 200 hPa. As shown in Figure 7(c) and (d), the similar Taylor Diagram is obtained when NCEP reanalysis is used as the reference, which suggests that the two reanalysis data are generally in good consistency. One exception is specific humidity at 850 hPa, as discrepancy exists in either correlation efficient or standard deviation, which demonstrates that water vapor is of great uncertainty even for reanalysis data.

5 Sensitivity experiment

As discussed in Section 3, the overestimated convective rainfall and underestimated stratiform rainfall by Tiedtke scheme is probably due to the unmatched stratiform scheme, but not Tiedtke scheme itself. In order to confirm this speculation, we deliberately evaporate the cloud liquid water and sublimate the cloud ice back into water vapor for the purpose of moistening environment humidity. As shown in Figure 8, the observed stratiform precipitation centers along ITCZ are successfully reproduced, and the rainfall is effectively intensified. Accordingly, the proportion of stratiform precipitation and the intensity of latent heating are also improved.

6 Summary and discussion

In this study, the performances of two cumulus convection schemes of the latest SAMIL are compared based on several observation data. The main conclusions are as follows:

(1) Convective rainfall is excessively overestimated by Tiedtke scheme, especially in the West Pacific Ocean. On the contrary, stratiform precipitation is underestimated compared with TRMM observation. However, the simulation by Manabe scheme is much closer to the observation, though rain bands in BOB spread eastward and northward associated with unrealistic strong precipitation downstream of the Tibet Plateau. Furthermore, the proportion of strati-

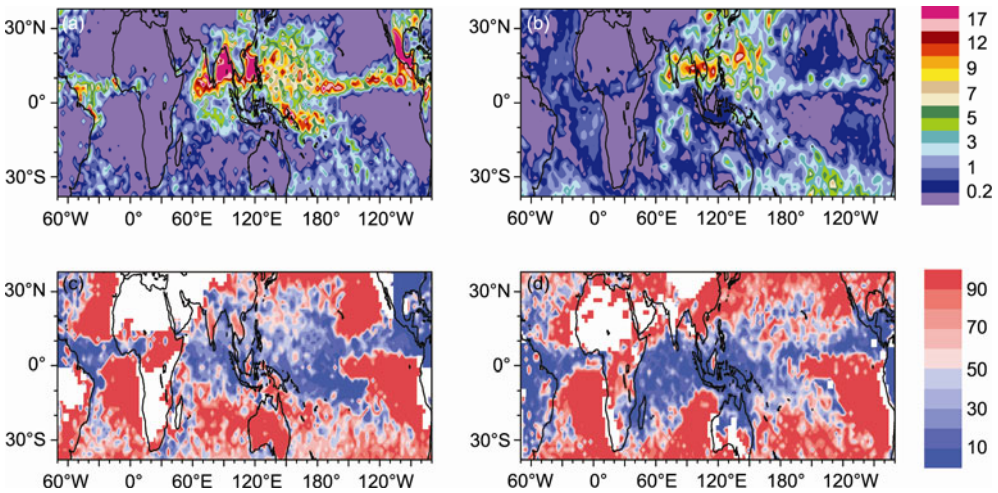

Figure 8 Precipitation distribution and stratiform rainfall proportion by modified Tiedtke scheme: convective rainfall (a), stratiform rainfall (b), stratiform rainfall proportion in JJA (c) and DJF (d).

form rainfall is well simulated by Manabe scheme, which is within the range of observation. The overestimated convective rainfall as well as underestimated stratiform rainfall by Tiedtke scheme leads to a low value of stratiform rainfall proportion. As a result, Tiedtke scheme fails in reproducing the stratiform rainfall shift with the seasons.

(2) The latent heating structure shows that Tiedtke scheme has an advantage over Manabe scheme, as the maximum convective latent heating near middle of troposphere is well reproduced. Moreover, the stratiform latent heating structure is also well simulated with warming above freezing level and cooling beneath freezing level. As for Manabe scheme, the simulated maximum convective latent heating lies near 700 hPa, lower than the observation. Additionally, the warming induced by stratiform latent heating extends to the whole vertical levels, which is unreasonable in comparison with observation.

(3) Taylor diagram further indicates that Tiedtke scheme is better than Manabe scheme as a higher correlation between model output and observation data is achieved when Tiedtke scheme is employed.

(4) The poor performance of Tiedtke scheme on the stratiform rainfall simulation is probably due to the unmatched stratiform scheme, in which the detrained water substance during convective process is not considered. The above speculation is verified through an established sensitivity experiment. Thence, a new cloud microphysical scheme that favors the current convective scheme is desirable. The performance of the later improved model will be analyzed and discussed elsewhere.

This work was supported by Special Fund Project of the Ministry of Science and Technology (Grant No. GYHY200806006), Knowledge Innovation Program of the Chinese Academy of Sciences (Grant No. KZCX2-YW-Q11-01), and National Natural Science Foundation of China (Grant Nos. 40925015, 40875034 and 40821092).

1 Smagorinsky J. On the inclusion of moist-adiabatic processes in numerical prediction models. Beitr Dtsch Wetterdien, 1956, 5: 82–90
2 Manabe S, Smagorinsky J, Strickler R. Simulated climatology of a general circulation model with a hydrologic cycle. Mon Weather Rev, 1965, 93: 769–798
3 Kuo H L. On formation and intensification of tropical cyclones through latent heat release by cumulus convection. J Atmos Sci, 1965, 22: 40–63
4 Arakawa A, Schubert W H. Interaction of a cumulus cloud ensemble with the large-scale environment: Part I. J Atmos Sci, 1974, 31: 674–701
5 Tiedtke M. A comprehensive mass flux scheme for cumulus parameterization in large-scale models. Mon Weather Rev, 1989, 117: 1779–1800
6 Wang J J, Zhou B, Guo X R. Numerical study of characteristics of condensational heating rates and their impacts of mesoscale structures of torrential rain simulations (in Chinese). Acta Meteorol Sin, 2005, 63: 405–417
7 Cheng A N, Chen W, Huang R H. Influence of convective parameterization schemes on climate numerical simulation (in Chinese). Chin J Atmos Sci, 1998, 22: 814–824
8 Cao J, Zhang X N, You Y L, et al. Applicability of cumulus convective parameter schemes in RegCM3 to the rainfall over the Longitudinal Range-Gorge Region. Chin Sci Bull, 2007, 52(Suppl): 115–121
9 Liu Y M, Guo L, Wu G X, et al. Sensitivity of ITCZ configuration to cumulus convective parameterizations on an aqua planet. Clim Dyn, 2010, 34: 223–240
10 Neale R B, Richter J H, Jochum M. The impact of convection on ENSO: From a delayed oscillator to a series of events. J Clim, 2008, 21: 5904–5924
11 Jia X L, Li C Y. Sensitivity of numerically simulated tropical intra-seasonal oscillations to cumulus schemes (in Chinese). Acta Meteorol Sin, 2007, 65: 837–855
12 Li J D, Liu Y M, Sun Z, et al. The impacts of the radiation and cumulus convective parameterization on the radiation fluxes in SAMIL (in Chinese). Acta Meteorol Sin, 2009, 67: 355–369
13 Arteta J, Marécal V, Rivière E D. Regional modeling of tracer transport by tropical convection—Part 1: Sensitivity to convection parameterization. Atmos Chem Phys, 2009, 9: 7081–7100
14 Lin J, Mapes B, Zhang M, et al. Stratiform precipitation, vertical heating profiles, and the Madden-Julian Oscillation. J Atmos Sci, 2004, 61: 296–309
15 Wu G X, Zhang X H, Liu H, et al. Global Ocean-Atmosphere-Land system model of LASG (GOALS/LASG) and its performance in simulation study (in Chinese). J Appl Meteorol Sci, 1997, 8(Supp1):

15–28
16 Wang Z Z, Wu G X, Liu P, et al. The development of GOALS/LASG AGCM and its global climatological features in climate simulation I: Influence of horizontal resolution (in Chinese). J Trop Meteorol, 2005, 21: 225–237
17 Wang Z Z, Yu R C, Wang P F, et al. The development of GOALS/LASG AGCM and its global climatological features in climate simulation II: The increase of vertical resolution and its influences (in Chinese). J Trop Meteorol, 2005, 21: 238–247
18 Wu T W, Liu P, Wang Z, et al. The performance of atmospheric component model R42L9 of GOALS/LASG. Adv Atmos Sci, 2003, 20: 726–742
19 Wu T W, Wu G X, Wang Z Z, et al. Simulation of the climate mean state in the GOALS/LASG model (in Chinese). Acta Meteorol Sin, 2004, 62: 20–31
20 Edwards J M, Slingo A. Studies with a flexible new radiation code. I: Choosing a configuration for a large-scale model. Q J R Meteorol Soc, 1996, 122: 689–720
21 Slingo J M. A cloud parameterization scheme derived from GATE data for use with a numerical model. Q J R Meteorol Soc, 1980, 106: 747–770
22 Slingo J M. The development and verification of a cloud prediction scheme for the ECMWF model. Q J R Meteorol Soc, 1987, 113: 899–927
23 Dai F S. Impacts of low-level cloud over the eastern Pacific Ocean on the Double ITCZ in an ocean-atmosphere coupled model: Diagnostic analyses based on LASG FGCM-0 (in Chinese). Dissertation for the Doctoral Degree. Beijing: Institute of Atmospheric Physics, Chinese Academy of Sciences, 2003
24 Bao Q, Liu Y M, Zhou T J, et al. The sensitivity of the spectral atmospheric general circulation model of LASG/IAP to the land process (in Chinese). Chin J Atmos Sci, 2006, 30: 1077–1090
25 Zhou T J, Yu R C, Wang Z Z, et al. Atmospheric circulation global model (SAMIL) and the coupled model (FGOALS-s) (in Chinese). Beijing: China Meteorological Press, 2005
26 Song X L. The evaluation analysis of two kinds of mass flux cumulus parameterizations in climate simulation (in Chinese). Dissertation for the Doctoral Degree. Beijing: Institute of Atmospheric Physics, Chinese Academy of Sciences, 2005
27 Liu Y M, Liu K, Wu G X. The impacts of the cumulus convective parameterization on the atmospheric water-content and rainfall simulation in SAMIL (in Chinese). Chin J Atmos Sci, 2007, 31: 1201–1211
28 Nordeng T E. Extended versions of the convective parameterization scheme at ECMWF and their impact on the mean and transient activity of the model in the tropics. Technical Memorandum, 1994
29 Adler R F, Susskind J, Huffman G J, et al. The Version-2 Global Precipitation Climatology Project (GPCP) Monthly Precipitation Analysis (1979–Present). J Hydrometeorol, 2003, 4: 1147–1167
30 Xie P P, Arkin P A. Global precipitation: A 17-year monthly analysis based on gauge observations, satellite estimates and numerical model outputs. Bull Amer Meteorol Soc, 1997, 78: 2539–2558
31 Uppala S M, Kallberg P W, Simmons A J, et al. The ERA-40 re-analysis. Q J R Meteorol Soc, 2005, 131: 2961–3012
32 Kalnay E, Kanamitsu M, Kistler R, et al. The NCEP/ NCAR 40-year reanalysis project. Bull Amer Meteorol Soc, 1996, 77: 437–471
33 Wang Z Z, Yu R C, Bao Q, et al. A comparison of the atmospheric circulations simulated by the FGOALS-s and SAMIL (in Chinese). Chin J Atmos Sci, 2007, 31: 202–213
34 Houze R A. Observed structure of mesoscale convective systems and implications for large-scale heating. Q J R Meteorol Soc, 1989, 115: 425–461
35 Houze R A. Stratiform precipitation in regions of convection: A meteorological paradox? Bull Amer Meteorol Soc, 1997, 78: 2179–2196
36 Leary C A, Houze R A. The structure and evolution of convection in a tropical cloud cluster. J Atmos Sci, 1979, 36: 437–457
37 Cheng C P, Houze R A. The distribution of convective and mesoscale precipitation in GATE radar echo patterns. Mon Weather Rev, 1979, 107: 1370–1381
38 Roeckner E, Bauml G, Bonaventura L, et al. Part I: Model description. In: The Atmospheric General Circulation Model ECHAM5. Hamburg: Max Planck Institute for Meteorology, 2004
39 Liu Y M, Wu G X, Liu H, et al. The effect of spatially nonuniform heating on the formation and variation of subtropical high, Part III: Condensation heating and south Asia high and western Pacific subtropical high (in Chinese). Acta Meteor Sin, 1999, 57: 525–538
40 Li C Y. Low-frequency Oscillation in the Atmosphere (in Chinese). Beijing: China Meteorological Press, 1991
41 Taylor K E. Summarizing multiple aspect s of model performance in a single diagram. J Geophys Res, 2001, 106: 7183–7192